

NONLINEAR OPTICAL PHENOMENA

PACS numbers: 78.66.–w; 42.65.–k
DOI: 10.1070/QE2013v043n12ABEH015270

Optical limiting effects in nanostructured silicon carbide thin films

A.A. Borshch, V.N. Starkov, V.I. Volkov, V.I. Rudenko, A.Yu. Boyarchuk, A.V. Semenov

Abstract. **We present the results of experiments on the interaction of nanosecond laser radiation at 532 and 1064 nm with nanostructured silicon carbide thin films of different polytypes. We have found the effect of optical intensity limiting at both wavelengths. The intensity of optical limiting at $\lambda = 532$ nm ($I_{cl} \sim 10^6$ W cm^{-2}) is shown to be an order of magnitude less than that at $\lambda = 1064$ nm ($I_{cl} \sim 10^7$ W cm^{-2}). We discuss the nature of the nonlinearity, leading to the optical limiting effect. We have proposed a method for determining the amount of linear and two-photon absorption in material media.**

Keywords: *optical limiting, nanostructured films, silicon carbide, polytypes.*

1. Introduction

Optical limiting effects are of considerable interest for nonlinear optics and optoelectronics due to their potential for protection of eyes and sensitive detectors from intense laser radiation, as well as for the development of optical switches and light emission control devices in information systems of optical communication and computing.

Studies of the last fifteen years have led to the emergence of three classes of nonlinear optical materials that ensure optical limiting based on mechanisms of different nature, including the reverse saturated absorption responsible for the optical limiting in nanoparticles of noble metals [1], fullerenes [2] and phthalocyanines [3], two-photon and multiphoton absorption responsible for optical limiting in semiconductor structures [4, 5], and nonlinear scattering, which is implemented mainly in suspensions of absorbing nanoparticles in organic solvents [6].

In addition, there is a series of papers [7, 8] devoted to the study of the optical limiting effects in materials used in outer space, which are subjected to prolonged exposure to solar UV radiation, X-ray and radioactive radiation, as well as experience extreme changes in temperature, resulting not only in malfunctioning of optical elements, but also in their destruction.

The aim of this paper was to experimentally investigate the possibility of observing the effects of optical limiting in nanostructured thin films of various silicon carbide polytypes, i.e., a medium promising for use at extremely high and low temperatures under significant radiation loads and in a chemically active atmosphere [9–11].

2. Experiment

Nanostructured silicon carbide (SiC) films were produced by the original technique of direct deposition of silicon and carbon ions on quartz or sapphire substrates at a relatively low (less than 1500 °C) temperature [12]. This technique allows one to control the process of formation of a nanocrystalline film, and thus to obtain samples with different polytypes of silicon carbide α-SiC (21R, 27R), β-SiC (3C), and with a varying degrees of crystalline phase (from 20% to 100%) [13]. In our studies we used the samples of nanostructures of different polytypes of silicon carbide (3C, 21R, 27R), which possess varying degrees of crystallinity (up to 100%), the samples that have only an amorphous phase, and the samples that have been subjected to annealing at a temperature ~1000 °C, followed by etching.

Single crystal bulk silicon carbide, as is known [14], has a sharp fundamental absorption edge in the range of photon energies 2.4–3.4 eV, depending on the polytype. The absorption spectra of the nanostructured silicon carbide samples we have fabricated exhibit extended 'tails' of the states in the visible and near-IR regions of the spectrum (Fig. 1), indicating the presence of nanoparticles with different local levels in the band gap of the material. These are primarily surface defects of a developed nanoparticle surface, which itself is a single crystal defect generating the so-called Tamm levels. In addition, these states in the band gap can be associated with the presence (along with the main polytype of silicon carbide nanomaterials) of some percentage of other polytypes as well as by-products of synthesis in nanostructured samples. Thus, according to photoelectron spectroscopy [15], nanostructured films, apart from heterobound SiC atoms, also contain homobound atoms of silicon Si–Si and carbon C–C. In this case, at the substrate temperatures of 700–950 °C, silicon not bound to carbon crystallises into a nanocrystalline phase with crystallites similar in size to silicon carbide. It should be noted that the broad absorption band in the visible and near-IR regions, we observed in the spectra of silicon carbide nanoparticles, indicates that the concentration of these states is very high and they can form an impurity band inside the band gap.

A.A. Borshch, V.N. Starkov, V.I. Volkov, V.I. Rudenko, A.Yu. Boyarchuk Institute of Physics, National Academy of Sciences of Ukraine, prosp. Nauki 46, 03028 Kiev, Ukraine;
e-mail: borshch@iop.kiev.ua, val@iop.kiev.ua;
A.V. Semenov Institute for Single Crystals, National Academy of Sciences of Ukraine, prosp. Lenina 60, 61178 Kharkov, Ukraine;
e-mail: semenov@isc.kharkov.ua

Received 4 July 2013; revision received 30 September 2013
Kvantovaya Elektronika **43** (12) 1122–1126 (2013)
Translated by I.A. Ulitkin

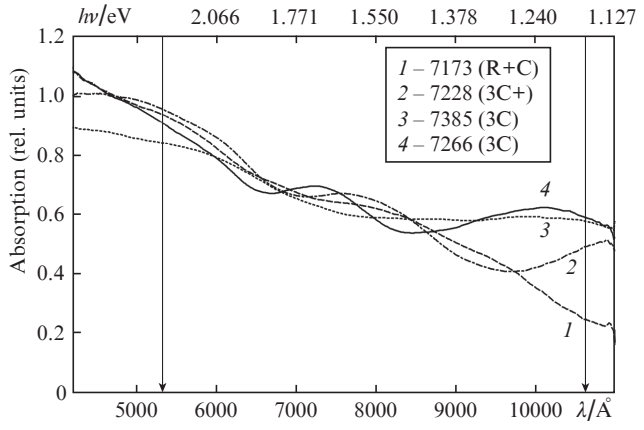

Figure 1. Absorption spectra of nanostructured thin films of different silicon carbide polytypes. Arrows here and in Fig. 2 show the wavelengths at which the experiment was performed.

Heat treatment of the synthesised nanostructured silicon carbide films by annealing at 1000 °C followed by etching leads to a significant depletion of these states in the band gap (Fig. 2).

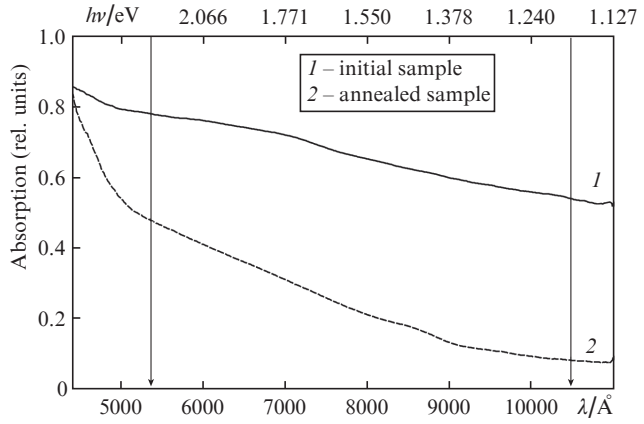

Figure 2. Absorption spectra of nanostructured silicon carbide films before (*1*) and after (*2*) annealing.

Optical limiting in nanostructured samples was studied according to the experimental scheme shown in Fig. 3, by using a pulsed passively *Q*-switched Nd:YAG laser with a pulse duration $\tau \approx 20$ ns at the fundamental wavelength of $\lambda = 1064$ nm and its second harmonic wavelength of $\lambda = 532$ nm. Single-mode laser radiation was focused with a lens having a focal length $F = 8.5$ cm on the sample, and the radiation emerging from the sample was collected with a similar lens and fed to a recording system. The input laser radiation intensity was controlled by an attenuator consisting of a $\lambda/2$ plate and a Glan prism. The laser pulse energy at the input and output of the circuit was measured using an automated multi-channel recording laser pulse system. The results were averaged by 20 pulses of the laser operating at a pulse repetition rate of 1 Hz.

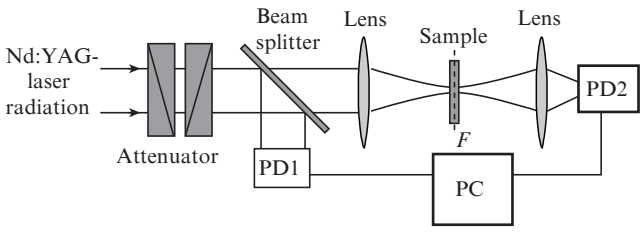

Figure 3. Scheme of the experimental setup.

3. Mathematical model

To analyse theoretically the experimental data on the transmission of the samples under study, we should first construct a mathematical model. The model is usually validated by comparing the results of computational and physical experiments.

Of no significant objection is the assumption that in an optical medium having a linear absorption, the relative change in light intensity $\Delta I/I$ in the samples along the direction of propagation z is proportional to the change in distance Δz:

$$\Delta I/I = -\alpha_0 \Delta z, \tag{1}$$

where α_0 is the linear absorption coefficient.

In semiconductors, along with the processes of linear absorption α_0, two-photon (or two-stage) absorption β and nonlinear scattering γ are present. Therefore, in equation (1), instead of the coefficient α_0, we should introduce the generalised extinction coefficient α, which is a function of the local intensity: $\alpha = \alpha(I)$. Because the methodology of an 'open' aperture used in research makes it impossible to register the scattering processes, allowance for the contribution of these processes in extinction in these experiments is not possible.

Thus, the generalised extinction coefficient can be given in the form

$$\alpha(I) = \alpha_0 + \beta(I), \tag{2}$$

where $I = I(z)$ is the local intensity of the laser radiation in W cm^{-2}.

Passing in (1) to the limit and taking expression (2) into account, the mathematical model can be written as an ordinary differential equation

$$\frac{\mathrm{d}I(z)}{\mathrm{d}z} = -[\alpha_0 + \beta I(z)]I(z). \tag{3}$$

The statement of the problem to determine the intensity of light in the sample along the propagation direction is completed by setting the boundary condition

$$I(z = 0) = I_{\text{in}}. \tag{4}$$

Thus, the Cauchy problem is formulated to determine the intensity of light in the sample, and its solution is obtained in an analytical form, which, in turn, made it possible to find an explicit expression for the dependence of the output intensity $I(z = a) = I_{\text{out}}$ on the input intensity I_{in}, i.e.,

$$I_{\text{out}} = \frac{I_{\text{in}}}{\exp(\alpha_0 a) - \mu[1 - \exp(\alpha_0 a)]I_{\text{in}}}, \tag{5}$$

where $\mu = \beta/\alpha_0$.

Expression (5) allows one to approximate confidently enough the data obtained by minimising the error of approximation of experimental data by the theoretical curves of mathematical modelling and, consequently, to obtain the values of the linear (α_0) and two-photon (β) absorption for all experimental samples.

4. Results and discussion

The experimental results of investigation of the optical limiting effect have shown that in the sample of silicon carbide, which is characterised mainly by an amorphous phase, the optical limiting effect both at the fundamental wavelength of a neodymium laser (λ= 1064 nm) and at its second harmonic (λ = 532 nm) is absent (Fig. 4). A similar result was obtained for the sample, which, due to additional annealing, consisted of a perfect (nearly 100%) nano-sized 3C-SiC (Fig.4).

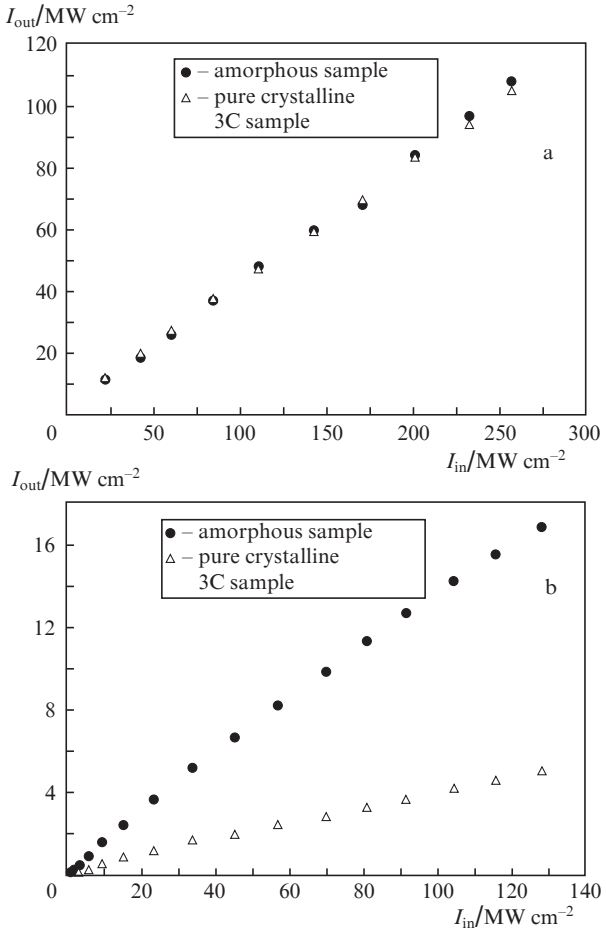

Figure 4. Intensities of radiation transmitted through the sample as functions of incident radiation intensity for the amorphous and 100% crystalline sample at λ = (a) 1064 and (b) 532 nm. The points show the experimental data and their vertical dimension approximately corresponds to the measurement error.

In contrast to these samples, all other nanostructured silicon carbide samples of different polytypes, obtained by direct ion deposition without any further treatment, exhibited a distinct effect of optical intensity limiting both at the fundamental wavelength of the neodymium laser (λ = 1064 nm), Fig. 5, and, at its second harmonic (λ = 532 nm), Fig. 6. One can see

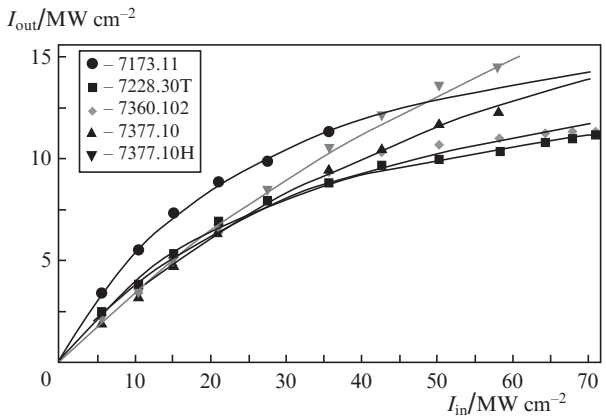

Figure 5. Output radiation intensities as functions of incident radiation intensity for the samples of different nanostructured silicon carbide polytypes at λ = 1064 nm. The points show the experimental data and their vertical dimension approximately corresponds to the measurement error. The curves represent the results of mathematical modelling.

from these figures that the intensity of limiting $I_{cl} \sim 10^6$ W cm^{-2} at λ = 532 nm is an order of magnitude less than the intensity of limiting at λ = 1064 nm.

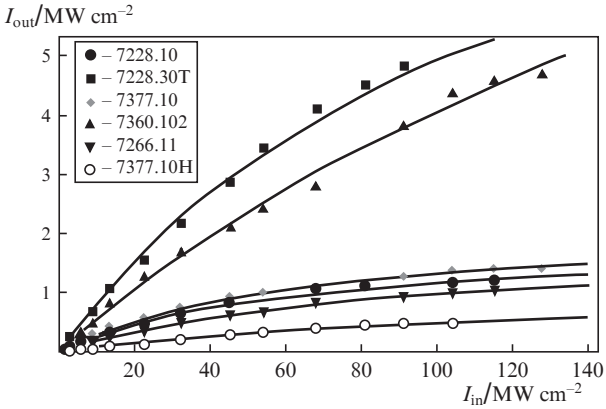

Figure 6. Output radiation intensities as functions of incident radiation intensity for the samples of different nanostructured silicon carbide polytypes at λ = 532 nm. The points show the experimental data and their vertical dimension approximately corresponds to the measurement error. The curves represent the results of mathematical modelling.

We performed an analysis of the experimental data of the samples under study in which we observed the effect of optical intensity limiting using our mathematical model. After averaging the intensity of the laser beam in Gaussian spatial and temporal (τ = 20 ns) profiles [16] and using expression (5), we were able to reliably approximate the experimental data by the results of the mathematical model based on the minimisation of the approximation error, which made it possible to obtain the values of the linear and nonlinear absorption for all experimental samples. The points in Figs 5 and 6 show the experimental data, i.e., dependences of the transmitted radiation intensity I_{out} on the incident intensity I_{in} of the investigated samples of nanostructured silicon carbide at λ = 1064 nm (Fig. 5) and λ = 532 nm (Fig. 6). The curves in these figures are the result of mathematical modelling. Table 1 shows the main parameters of the investigated samples, as

Table 1.

Sample No	Polytype	λ_{ex}/nm	Thickness/nm	α/cm^{-1}	β/cm kW^{-1}	Relative error (%)
7173.11	27R+3C	1064	0.67	4247	0.6593	1.7
		532		56905	0.8904	4.1
7228.10	3C	1064	1.0	33546	0.5383	5.0
		532		34092	0.6482	2.5
7228.30T	3C	1064	1.0	6039	0.4625	2.1
		532		23946	0.2241	3.5
7266.11	3C	1064	1.0	7185	0.09642	4.4
		532		33847	0.5561	1.3
7360.102	3C	1064	0.4	18098	0.9548	4.6
		532		72613	0.2745	3.6
7377.10	21R+3C	1064	0.55	17199	0.3823	1.5
		532		70904	0.7863	2.1
7377.10H	3C	1064	0.5	19435	0.2769	2.2
		532		93468	0.99395	2.6
7000	–	1064	1.4	4993	–	Amorphous sample
		532		14188	–	
7300.11	3C	1064	0.4	18098	–	Perfect cristallinity
		532		72613	–	

well as the values of α_0 and β obtained by minimising the error of approximation of the experimental data by the results of mathematical modelling.

To confirm the validity of the proposed mathematical model and the accuracy of determining the coefficients of linear and nonlinear absorption, we have independently measured the linear and nonlinear absorption in some of our samples using the known z-scan technique [4], in which the laser radiation transmission is measured as a function of position of the sample with respect to the point of radiation focusing, $z = 0$ (i.e., as a function of radiation intensity on the sample). The diameter of the laser beam in front of the lens with $F = 14$ cm was equal to 2 mm. Measurements were carried out at laser radiation wavelengths of 1064 and 532 nm and a pulse duration $\tau = 20$ ns. Typical experimental curves (z-scans), obtained for one of the investigated samples (No. 7377.10N) are shown in Fig. 7. The linear and nonlinear absorption coefficients for sample No. 7377.10N obtained in this experiment are as follows: $\alpha_0 = 19359$ ($\pm 10\%$) cm^{-1}, $\beta = 0.2588$ ($\pm 15\%$) cm kW^{-1} at $\lambda = 1064$ nm and $\alpha_0 = 93630$ ($\pm 10\%$) cm^{-1}, $\beta = 0.9533$ ($\pm 15\%$) cm kW^{-1} at $\lambda = 532$ nm. In minimising the approximation error of the experimental data by the results of mathematical modelling (see Table 1), we have $\alpha_0 = 19435$ cm^{-1}, $\beta = 0.2769$ cm kW^{-1} at $\lambda = 1064$ nm and $\alpha_0 = 93468$ cm^{-1}, $\beta = 0.99395$ cm kW^{-1} at $\lambda = 532$ nm, which is consistent with the values obtained experimentally.

Thus, we have confirmed the validity of the proposed mathematical model and proposed a method for determining the linear and nonlinear absorption in material media.

The analysis performed has shown that nonlinear absorption that leads to the effect of optical intensity limiting is associated with the levels located in the band gap of the material of silicon carbide nanoparticles, which are absent in samples with an amorphous phase and largely suppressed in samples with an almost 100% crystalline phase. These levels can obviously take part in two-stage absorption both as the ground states, from which the carriers can be injected in two stages in the conduction band, and intermediate states. Besides, the nonlinear absorption should be supplemented by absorption of radiation by excited nonequilibrium carriers, which will also be nonlinear because

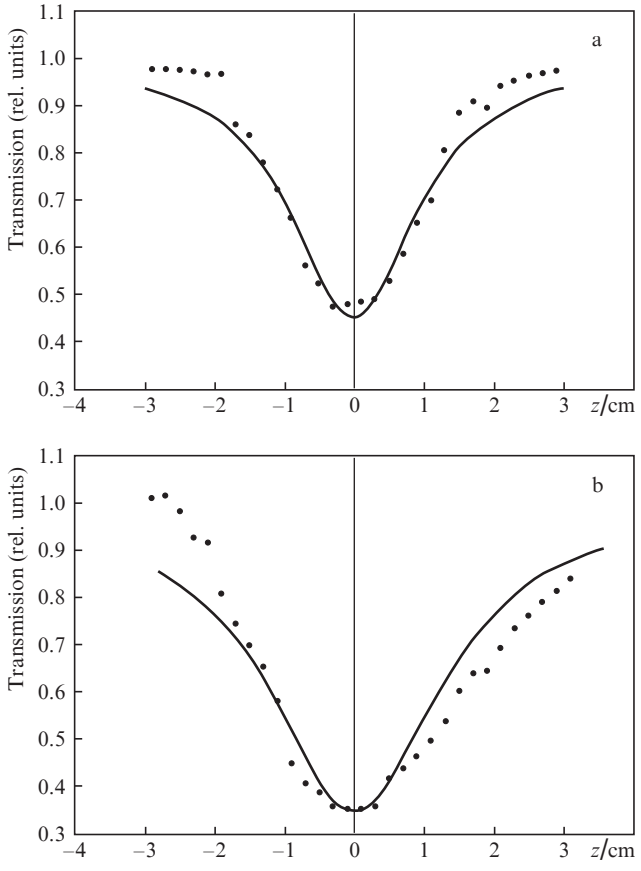

Figure 7. Experimental curves of z-scanning of sample No. 7377.10H (open aperture) at λ = (a) 1064 nm and (b) 532 nm.

the concentration of these carriers increases quadratically with intensity. The two-stage mechanism of nonlinear absorption is supported by the data of the measurement of the nonlinear absorption coefficient itself, β. Indeed, in the case of two-photon absorption, the nonlinearity coefficient at $\lambda = 532$ nm must always be greater than at $\lambda = 1064$ nm because of the greater photon energy at $\lambda = 532$ nm, and hence a larger energy band gap of the excited levels. In the case of two-stage transitions, such a condition is not mandatory, since of importance here is the concentration of the intermediate local states in a certain area of the band gap. As can be seen from Table 1, in samples No. 7228.30T and No. 7360.102 the nonlinear absorption β at $\lambda = 1064$ nm substantially higher than that at $\lambda = 532$ nm.

Thus, the results obtained show that the nonlinear absorption leading to optical intensity limiting is most likely due to the two-step excitation of charge carriers from the local levels in the band gap into the conduction band and due to the absorption by excited nonequilibrium carriers.

5. Conclusions

The results presented demonstrate that in nanostructured films of wide bandgap silicon carbide semiconductors there arises an optical nonlinearity in the visible and near-IR ranges, leading to the effect of optical limiting of the output intensity. The nonlinearity is due to the nonlinear photogeneration of carriers from local defect levels located in the band gap of the material into the conduction band and to the subsequent absorption of radiation by excited nonequilibrium carriers.

These effects observed in the nanostructured silicon carbide films are promising for the development of optical switches and radiation limiters and can be used at extremely high and low temperatures under significant radiation loads and in a chemically active atmosphere.

References

1. Ganeev R.A., Ryasnyansky A.V., Kamalov S.R., Kodyrov M.K., Usmanov T. *J. Phys. D: Appl. Phys*., **34**, 1602 (2001).
2. Tutt L.W., Kost A. *Nature*, **356**, 225 (1992).
3. Fuqua P.D., Mansour K., Alvarez D., Marder S.R., Perry J.W., Dunn B. *Proc. SPIE Int. Soc. Opt. Eng.*, **1758**, 499 (1992).
4. Sheik-Bahae M., Said A.A., Wei T.H., Hagan D.J., Van Stryland E.W. *IEEE J. Quantum Electron*., **26**, 760 (1990).
5. Hagan D.J., Van Stryland E.W., Wu Y.Y., Wei T.H., Sheik-Bahae M., Said A.A., Kamjou Mansour, Young J., Soileau M.J. *Proc. SPIE Int. Soc. Opt. Eng*, **1105**, 103 (1989).
6. Vicent D. *Nonlinear Opt*., **21** (1–4), 413 (1999).
7. Townsend J.A., Hansen P.A., McClendon M.W., de Groh K.K., Banks B.A. *High Perform. Polym.*, **11**, 1 (1999).
8. Chen Y., Gin Y., Doyle J., He N., Zhuang K., Bai J., Blau W.J. *J. Nanosci. Nanotechnol.*, **7**, 1268 (2007).
9. Borzyak P.G., Borshch A.A., Brodin M.S., Volkov V.I., Tarashchenko D.T. Inventor's Certificate No. 528802. *Bulletin of Inventions*, No. 9, 223 (1977).
10. Borshch A.A., Brodin M.S., Volkov V.I., Tarashchenko D.T. *Kvantovaya Elektron*., **4** (3), 646 (1977) [*Sov. J. Quantum Electron*., **7** (3), 358 (1977)].
11. Andrievskii R.A. *Usp. Khim*., **78**, 889 (2009).
12. Semenov A.V., Lapin A.V., Puzikov V.M. *Poverkhnost', Rentgenovskie, Sinkhrotronnye i Neitronnye Issledovaniya*, **9**, 99 (2004).
13. Semenov A.V., Skorik S.N., Lopatin A.V., Puzikov V.M., Baumer V.N., Mateichenko P.V. *Poverkhnost', Rentgenovskie, Sinkhrotronnye i Neitronnye Issledovaniya*, **7**, 58 (2010).
14. *Semiconductors: Physics of Group IV Elements and III-V Compounds*, in: Madelung O., Schulz M., Weiss H. (Eds) Landolt-Börnstein New Series, Vol. III/17a (Berlin: Springer, 1982).
15. Semenov A.V., Puzikov V.M., Dobrotvorskaya M.V., Fedorov A.G., Lopin A.V. *Thin Solid Films*, **516**, 2899 (2008).
16. Borshch A.A., Brodin M.S., Krupa N.N., Lukomskii V.P., Pisarenko V.G., Petropavlovskii A.I., Chernyi V.V. *Zh. Eksp. Teor. Fiz*., **75**, 82 (1978).